JACS
JOURNAL OF THE AMERICAN CHEMICAL SOCIETY
pubs.acs.org/JACS
Article

Vanadium Alkylidyne Initiated Cyclic Polymer Synthesis: The Importance of a Deprotiovanadacyclobutadiene Moiety

Mehrafshan G. Jafari, John B. Russell, Hanna Lee, Bimal Pudasaini, Digvijayee Pal, Zhihui Miao, Michael R. Gau, Patrick J. Carroll, Brent S. Sumerlin,* Adam S. Veige,* Mu-Hyun Baik,* and Daniel J. Mindiola*

Cite This: J. Am. Chem. Soc. 2024, 146, 2997−3009
Read Online

ACCESS | Metrics & More | Article Recommendations | Supporting Information

ABSTRACT: Reported is the catalytic cyclic polymer synthesis by a 3d transition metal complex: a V(V) alkylidyne, [(dBDI)V≡C^{t}Bu(OEt$_2$)] (**1−OEt$_2$**), supported by the deprotonated β-diketiminate dBDI^{2-} (dBDI^{2-} = ArNC(CH$_3$)CHC(CH$_2$)NAr, Ar = 2,6-^{i}Pr$_2$C$_6$H$_3$). Complex **1−OEt$_2$** is a precatalyst for the polymerization of phenylacetylene (PhCCH) to give cyclic poly(phenylacetylene) (*c*-PPA), whereas its precursor, complex [(BDI)V≡C^{t}Bu(OTf)] (**2−OTf**; BDI$^-$ = [ArNC(CH$_3$)]$_2$CH, Ar = 2,6-^{i}Pr$_2$C$_6$H$_3$, OTf = OSO$_2$CF$_3$), and the zwitterion [((C$_6$F$_5$)$_3$B−dBDI)V≡C^{t}Bu(OEt$_2$)] (**3−OEt$_2$**) exhibit low catalytic activity despite having a neopentylidyne ligand. Cyclic polymer topologies were verified by size-exclusion chromatography (SEC) and intrinsic viscosity studies. A component of the mechanism of the cyclic polymerization reaction was probed by isolation and full characterization of 4- and 6-membered metallacycles as model intermediates. Metallacyclobutadiene (MCBD) and deprotiometallacyclobutadiene (dMCBD) complexes (dBDI)V[C(^{t}Bu)C(H)C(^{t}Bu)] (**4−^{t}Bu**) and (BDI)V[C(^{t}Bu)CC(Mes)] (**5−Mes**), respectively, were synthesized upon reaction with bulkier alkynes, ^{t}Bu− (^{t}BuCCH) and Mes−acetylene (MesCCH), with **1−OEt$_2$**. Furthermore, the reaction of the conjugate acid of **1−OEt$_2$**, [(BDI)V≡C^{t}Bu(OTf)] (**2−OTf**), with the conjugated base of phenylacetylene, lithium phenylacetylide (LiCCPh), yields the doubly deprotio-metallacycle complex, [Li(THF)$_4$]{(BDI)V[C(Ph)CC(^{t}Bu)CC(Ph)]} (**6**). Protonation of the doubly deprotio-metallacycle complex **6** yields **6−H$^+$**, a catalytically active species toward the polymerization of PhCCH, for which the polymers were also confirmed to be cyclic by SEC studies. Computational mechanistic studies complement the experimental observations and provide insight into the mechanism of cyclic polymer growth. The noninnocence of the supporting dBDI^{2-} ligand and its role in proton shuttling to generate deprotiometallacyclobutadiene (dMCBD) complexes that proposedly culminate in the formation of catalytically active V(III) species are also discussed. This work demonstrates how a dMCBD moiety can react with terminal alkynes to form cyclic polyalkynes.

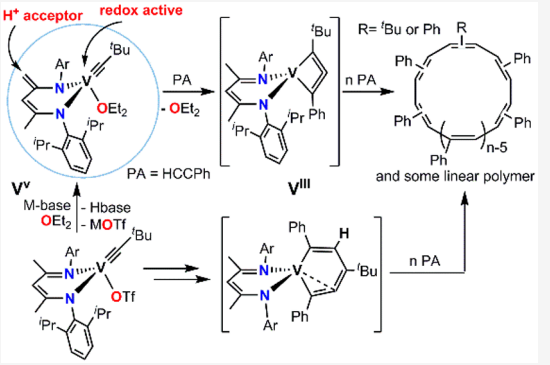

INTRODUCTION

Polyalkynes are an important family of conjugated polymers known for their high and tunable electrical conductivity. These polymers possess not only excellent conductivity but also intriguing physical characteristics such as nonlinear optical properties,[1] gas permeability,[2] and many other outstanding features. Consequently, they hold great promise for applications as organic conductive polymers,[3] optical limiters,[1,4] and membranes for gas separation.[2] Substituted polyacetylenes serve as substrates for synthesizing a diverse range of polymers through postpolymerization modifications.[5] Polymers with modified topologies offer potential advantages for fabricating specific materials and coatings, modifying surface properties, and facilitating drug delivery. Among these topologies, cyclic polymers are particularly interesting due to their unique properties arising from the absence of polymer chain termination points.[4,6] These "endless" and "continuous" polymers exhibit lower viscosity,[7] higher thermostability, shorter radii, smaller hydrodynamic volume,[8] higher refractive index, different reptation in solution media,[9] and distinctive surface properties.[10,11] Despite the excitement surrounding cyclic polymers, only a few reports described the polymerization of alkynes to access cyclic polyalkynes,[12,13] due to the challenging entropic penalties associated with their formation. Apart from the more traditional ring-closing metathesis (RCM) methodology, which has its own challenges and drawbacks,[14] new methods developed by Grubbs, Veige, and

Received: July 28, 2023
Revised: December 6, 2023
Accepted: December 12, 2023
Published: January 25, 2024

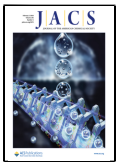

https://doi.org/10.1021/jacs.3c08149
J. Am. Chem. Soc. 2024, 146, 2997−3009

Scheme 1. Top: Definitions for relevant organometallic fragments discussed in this work. Left: Cyclic polymerization involving the ring-expansion metathesis of a cyclic olefin with a tethered carbene (A, Enene pathway), ring-expansion metathesis of a cyclic olefin with a carbyne (B, Ynene pathway), or subsequent alkyne insertion using a metallacyclopropene (C, Alkyne insertion and ring-expansion pathway). Right: Our study showing [2+2]-cycloaddition of a terminal alkyne with an alkylidyne followed by proton shuttling to form a bent allene, which upon structural rearrangement and subsequent [2+2]-cycloadditions result in the formation of cyclic and linear polymer mixture (D).

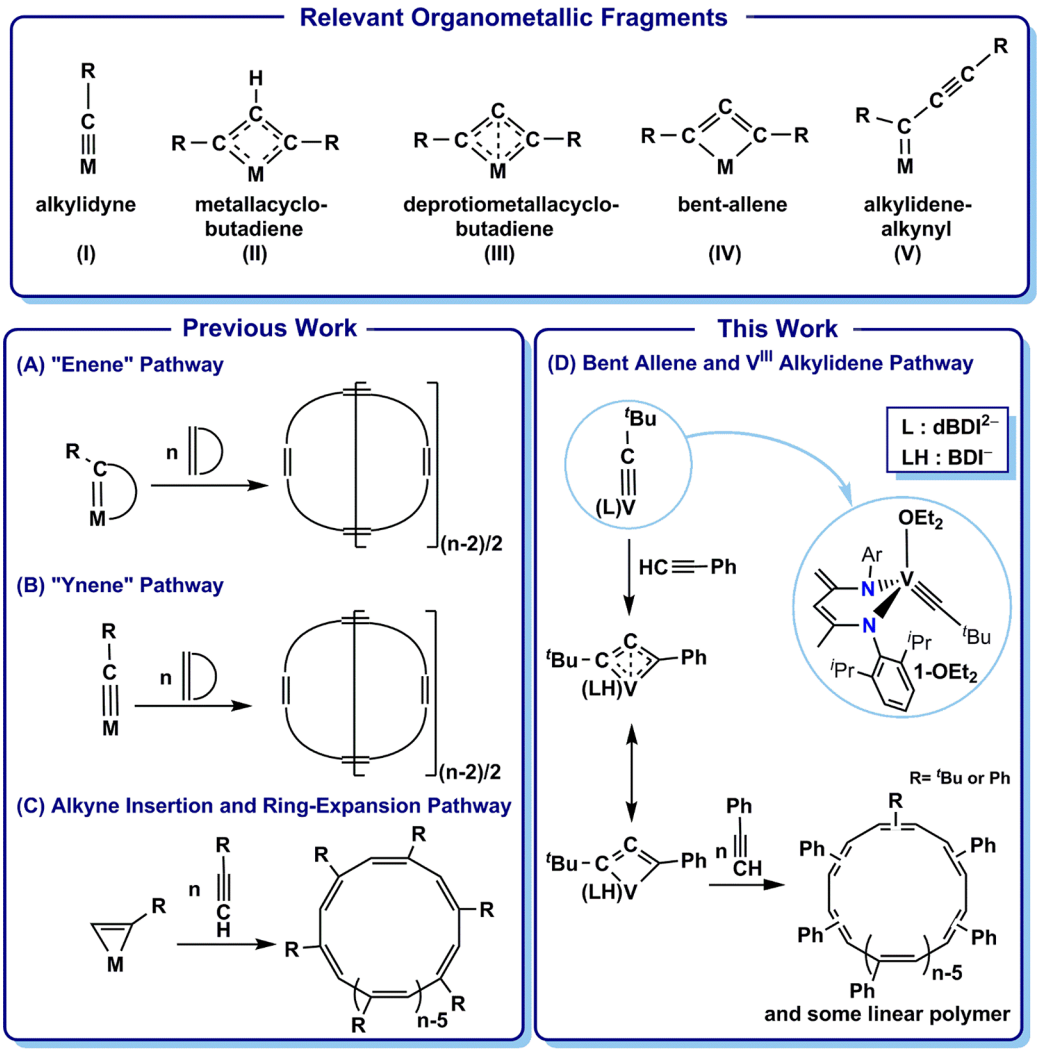

co-workers established direct access to cyclic polyalkenes via the ring expansion metathesis polymerization (REMP), highlighted as the Enene pathway in Scheme 1A.[11,15] Veige and his team employed a [W^{VI}] alkylidyne (top of Scheme 1, I) precursor and invoked an ynene mechanism to generate cyclic polynorbornene (Scheme 1B),[16] while Maeda and co-workers have shown that alkyne adducts of Mo, W, and Ta can also catalyze the cyclic polymerization of internal alkynes presumably via an insertion and ring-expansion pathway (Scheme 1C). However, many aspects of these mechanisms remain to be fully understood.[17] A recent discovery by our team has lead to the cyclic polymerization of phenylacetylene from bent-allenes (Scheme 1, IV), on the Ti and V metal center.[45] Apart from these limited examples, a synthetic methodology for the cyclic polymerization of alkynes using a 3d transition-metal-alkylidyne has yet to be established. Moreover, the limited mechanistic information available for polymer growth hampers future catalyst design and optimization. In this work, we evaluate the catalytic activity of the only reported d^0 vanadium alkylidynes[18,19] for cyclic polymerization of phenylacetylene (PA) and present a comprehensive mechanistic investigation of how deprotio-metallacyclobutadienes (dMCBDs) (top of Scheme 1, III) critically contribute to alkylidene formation and polymer propagation.

Scheme 1D presents a novel route for obtaining cyclic polymers of alkynes. The initiation step involves a [2+2]-cycloaddition of [M≡C] and [C≡C] bonds, followed by an unprecedented bimolecular deprotonation of the metallacyclobutadiene (MCBD) (top of Scheme 1, II). During this deprotonation process, the proton is transferred to the $dBDI^{2-}$ ligand ($dBDI^{2-}$ = $ArNC(CH_3)CHC(CH_2)NAr$, Ar = 2,6-$^{i}Pr_2C_6H_3$). Experimental evidence is provided to illustrate how proton shuttling influences the reaction direction, thereby discouraging cycloreversion and alkyne cross-metathesis. The formation of a deprotiometallacyclobutadiene (dMCBD) (Scheme 1D) allows the vanadacycle to rearrange via a proposed bent allene (top of Scheme 1, IV) and a V(III) alkylidene-alkynyl (top of Scheme 1, V). This alkylidene-

https://doi.org/10.1021/jacs.3c08149
J. Am. Chem. Soc. 2024, 146, 2997−3009

alkynyl species can then propagate via metathesis polymerization of PA. By preparing similar analogues of these metallacycles, including alternative routes to a precatalyst with a highly anionic 6-membered ring formed from the net fusion of two alkynes and the V≡C^{t}Bu moiety (compound **6**), we demonstrate the likeliness of these intermediates participating in polymer initiation and propagation. Computational studies provide insights into the formation of dMCBD and its subsequent rearrangement to an alkylidene-alkynyl, which ultimately allows for the formation of cyclic poly(phenylacetylene) (*c*-PPA). This work is the first systematic demonstration of how 3d transition-metal−alkylidynes can facilitate the formation of *c*-PPA.

RESULTS AND DISCUSSION

Polymerization Reactions and Polymer Topological Studies. This study was motivated by previous findings in 2004, where complex **2−OTf**, in the presence of 1 equiv of LiCH$_2$^{t}Bu, polymerized PA to yield what was initially assumed to be linear poly(phenylacetylene), (*l*-PPA).[18] Considering the report by Veige et al., which demonstrated that an alkylidyne can initiate the polymerization of norbornene[15] and alkynes[16] to give cyclic polymers, it seemed plausible to re-examine whether **2−OTf** could also produce cyclic polymers. Thus, three V(V) alkylidynes (Figure 1) were tested for their activity

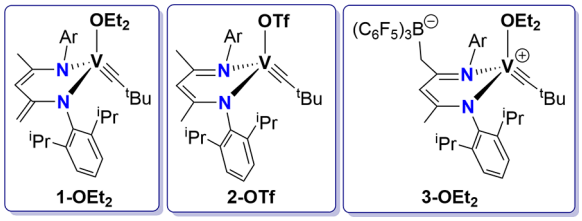

Figure 1. V(V) alkylidynes tested for the polymerization of phenylacetylene (PA).

in the polymerization of PA. Among these three species, **1−OEt$_2$**, a V(V) alkylidyne complex bearing a deprotonated *β*-diketiminate (dBDI^{2-}) ligand, exhibited the highest yield and most promising reactivity for the polymerization of PA. Various reaction conditions with **1−OEt$_2$** were screened (Table 1, entries 1−10), and it was determined that a 1:1000 ratio of [**1−OEt$_2$**]:[PA] in toluene provides the best yield (94%) and rate (12 h) of polymers with a molecular weight (M_w) on the order of 10^5 Da (entry 10). In comparison, catalysts **2−OTf** and **3−OEt$_2$** offer yields below 25% and 5%, respectively, even with higher catalyst loadings (Table 1, entries 11 and 12). The higher reactivity of **1−OEt$_2$** and **3−OEt$_2$** can be attributed to the higher lability of Et$_2$O compared to triflate, as the elimination of Et$_2$O may facilitate the initial [2+2]-cycloaddition or activation of the alkyne and alkylidyne. Computational studies suggest that the dissociation of Et$_2$O requires about 20.7 kcal/mol of Gibbs free energy to form the transient and unsaturated complex [(dBDI)V≡C^{t}Bu] {**1**} with an open coordination site, as indicated by B3LYP calculations (Figure S25). The energy required is not prohibitive for the subsequent coordination of PA and the initiation of polymerization. This finding suggests that weakly coordinated solvents are optimal. Indeed, toluene exhibited the best solvent performance for these reactions, whereas coordinating solvents, such as THF, effectively halted the polymerization. Another observation from the polymerization studies is that more concentrated reaction conditions yield better results as long as the viscosity of the reaction media still allows for vigorous and effective stirring (Table 1, entries 1 vs 2, 5 vs 6 vs 7, and 8 vs 9 vs 10).

To compare the obtained polymers with the anticipated cyclic topology, linear analogs of poly(phenylacetylene) were synthesized using (acac)Rh(COD) catalyst (acac$^-$ = [OC(CH$_3$)]$_2$CH, COD = C$_8$H$_{12}$).[20] The elution times of the PPA synthesized with the **1−OEt$_2$** catalyst and the standard *l*-PPA with similar molecular weights were compared by size-exclusion chromatography. The PPA prepared by **1−OEt$_2$** catalyst exhibited longer elution times compared to the linear analogs, which is consistent with the presence of *c*-PPA. This is expected since the cyclic topology is anticipated to have a smaller hydrodynamic volume compared to its linear counterpart (Figure 2A, refer to Table 1 for reaction conditions). However, the convergence of elution volumes for lower

Table 1. Selected Polymerization with Various Vanadium Catalysts[a]

entry	[PhCCH]:[Cat.]	Cat.	[PhCCH] (M)	reaction time (h)	reaction volume (mL)	conversion (%)[b]	$Đ$[c]	M_n (kDa)[c]
1	100	**1−OEt$_2$**	0.1	2	10	93	1.66	204
2	100	**1−OEt$_2$**	0.2	2	5	94	1.30	172
3	1000	**1−OEt$_2$**	0.2	2	10	15		
4	1000	**1−OEt$_2$**	0.2	4	10	21	1.80	181
5	1000	**1−OEt$_2$**	0.2	6	10	44	1.32	197
6	1000	**1−OEt$_2$**	0.4	6	5	62	1.48	140
7	1000	**1−OEt$_2$**	1.0	6	2	72	2.02	133
8	1000	**1−OEt$_2$**	0.2	12	10	69	1.48	93.5
9	1000	**1−OEt$_2$**	0.4	12	5	89	1.60	82.5
10	1000	**1−OEt$_2$**	1.0	12	2	94	1.64	62.9
11	100	**2−OTf**	0.5	20	2	23		
12	500	**3−OEt$_2$**	0.2	12	5	4		
13	∼1000	**6−H$^+$**	0.4	12	5	19	1.49	115
14	∼1000	**6−H$^+$**	1.0	12	2	37	1.48	108
15	∼10000	**6−H$^+$**	1.8	12	2	8		
16	∼8362	**6−H$^+$**	5.4	12	5	2	1.40	152.4

[a]All mentioned reactions have been performed in toluene and at room temperature. [b]Determined based on the mass of polymer after workup. [c]Measured and determined by SEC analysis, calibrated by polystyrene standards.

https://doi.org/10.1021/jacs.3c08149
J. Am. Chem. Soc. 2024, 146, 2997−3009

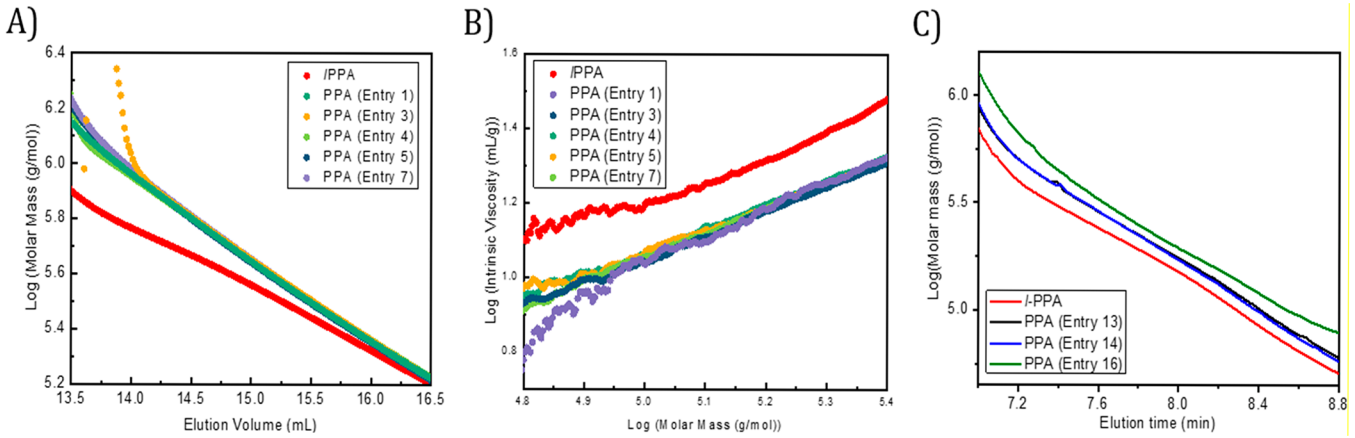

Figure 2. (A) Log(molar mass) vs elution volume for poly(phenylacetylene) samples (PPAs) (cf. Table 1 for reaction conditions). The red trace represents linear poly(phenylacetylene) prepared independently with (acac)Rh(COD) as the catalyst. (B) Mark–Houwink–Sakurada plot for the comparison of intrinsic viscosities over a wide range of molecular weights for linear and cyclic PPA (*l*-PPA and *c*-PPA) samples in THF at 35 °C. (C) Log(molar mass) vs elution volume of PPA synthesized with catalyst **6**–H^+ (cf. Table 1 for reaction conditions). The red trace represents *l*-PPA prepared independently with the catalyst (acac)Rh(COD).

Scheme 2. Left: (A) Synthesis of MCBD 4–^{t}Bu from 1–OEt_2 and ^{t}BuCCH. (B) Synthesis of the dMCBD 5–Mes from 1–OEt_2 and MesCCH. (C) Synthesis of the 6-membered metallacycle 6 via addition of 2 equiv of LiCCPh to 2–OTf. Center: (D) Dissociation of diethylether (Et_2O) from 1–OEt_2 followed by (E) [2+2]-cycloaddition of 1 and PA to form 4–Ph. (F) Bimolecular proton shuttling of 4–Ph to yield 5–Ph. (G) Various resonance structures of 5–Ph are shown, which can undergo structural change to afford a bent allene (5′–Ph) or an alkylidene-alkynyl species (5″–Ph).

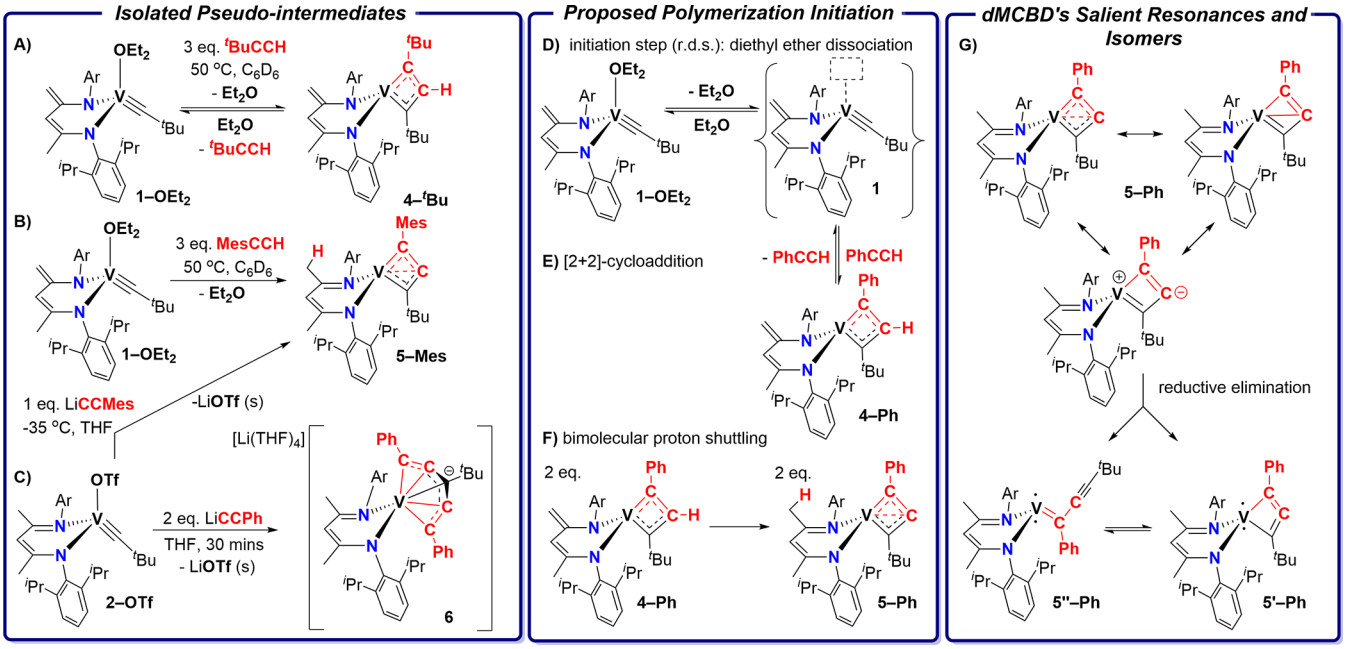

molecular weights suggests the possibility of trace *l*-PPA impurities in the *c*-PPA sample.

Further evidence supporting the cyclic topology for polymers synthesized with catalyst **1–OEt_2** is their lower intrinsic viscosities [η] throughout the molecular weight range compared to the linear analogs (Figure 2B).[12,21]

Reactivity of the Metal–Carbon Multiple Bond with Terminal Alkynes. Cross-metathesis reactions involving transition metal alkylidynes with internal alkynes are well-known,[22−25] leading to the formation of a MCBD intermediate (top of Scheme 1, II).[26,27] However, when metal alkylidynes react with terminal alkynes, a different reaction occurs: [2+2]-cycloaddition followed by β-CH abstraction results in the formation of the corresponding dMCBD (top of Scheme 1, III).[25,28−32] Interestingly, these dMCBD species initiate the formation of "unidentified" polymers through the expansion of the metallacyclic ring upon the addition of terminal alkynes.[28,30] Since the initial reports on the formation of dMCBDs,[29] there has been significant interest in their potential structural and electronic rearrangement to bent allenes (top of Scheme 1, IV) and alkylidenes with pendent alkynyl groups (top of Scheme 1, V).[30] In 1993, Mortreux and co-workers proposed that dMCBD intermediates rearrange to form an alkylidene-alkynyl motif capable of initiating alkyne metathesis polymerization, resulting in the formation of poly-alkynes.[33] However, the limited evidence for the polymer-

https://doi.org/10.1021/jacs.3c08149
J. Am. Chem. Soc. 2024, 146, 2997−3009

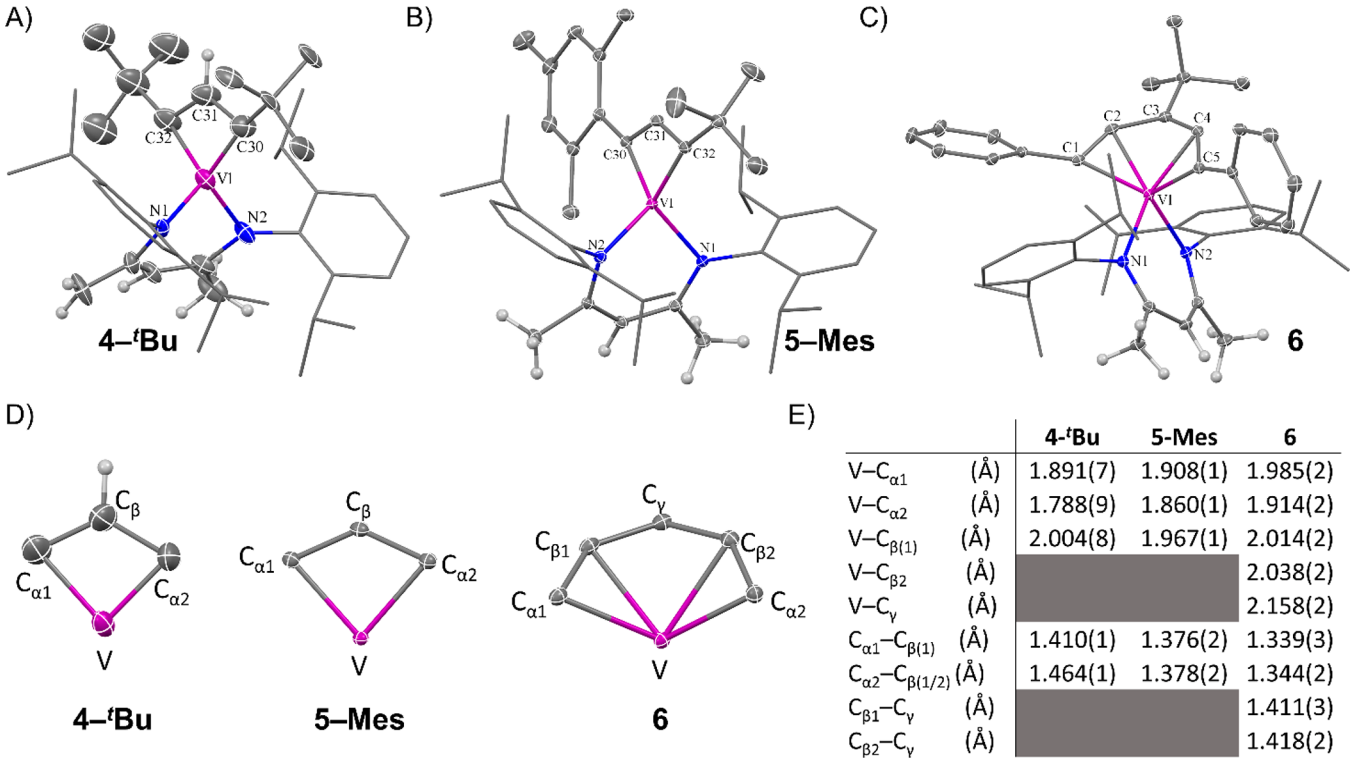

E)

		4-^{t}Bu	5-Mes	6
V–$C_{α1}$	(Å)	1.891(7)	1.908(1)	1.985(2)
V–$C_{α2}$	(Å)	1.788(9)	1.860(1)	1.914(2)
V–$C_{β(1)}$	(Å)	2.004(8)	1.967(1)	2.014(2)
V–$C_{β2}$	(Å)			2.038(2)
V–$C_{γ}$	(Å)			2.158(2)
$C_{α1}$–$C_{β(1)}$	(Å)	1.410(1)	1.376(2)	1.339(3)
$C_{α2}$–$C_{β(1/2)}$	(Å)	1.464(1)	1.378(2)	1.344(2)
$C_{β1}$–$C_{γ}$	(Å)			1.411(3)
$C_{β2}$–$C_{γ}$	(Å)			1.418(2)

Figure 3. Structural representation of (A) **4–^{t}Bu** with thermal ellipsoids at the 30% probability level. (B) **5–Mes** with thermal ellipsoids at the 50% probability level. (C) **6** with thermal ellipsoids at the 50% probability level. Hydrogen atoms, except for those relevant to the discussion, disordered aryl, and ^{t}Bu groups in **4–^{t}Bu**, cocrystallized hexane, and $Li^+(THF)_4$ counterion in **6** are all omitted for clarity. Ar groups on the ligand are shown in a capped stick style for simplicity. (D) A closer structural demonstration of metallacyclic motifs and Greek alphabetical label assignments. (E) Tabulated list of salient bond distances.

ization mechanism from Schrock alkylidynes and the insufficient characterization of the resulting polymers have impeded the full realization of the potential of these catalysts.[28,33,34]

As mentioned above, dMCBD complexes are synthesized via [2+2]-cycloaddition of terminal alkynes with tungsten and molybdenum alkylidynes,[25,28−32] followed by irreversible deprotonation assisted by the ancillary ligand, often resulting in dissociation of the conjugate acid. In our case, when utilizing the V alkylidyne **1–OEt$_2$** with a terminal alkyne such as phenylacetylene, we propose the formation of a similar MCBD species through [2+2]-cycloaddition, followed by deprotonation but without ligand dissociation. Such a transformation is possible since the dianionic supporting ligand ($dBDI^{2-}$) has the potential to support the V complex as a monoanionic BDI^- ligand after accepting a proton. To investigate the initiation steps, we examined the reactivity of **1–OEt$_2$** with other terminal alkynes containing sterically congested groups: (1) an alkyl-substituted terminal alkyne with a less acidic terminal alkynyl CH group, ^{t}Bu–acetylene (^{t}BuCCH) and (2) an aryl-substituted terminal alkyne with similar structure and terminal CH acidity to phenylacetylene, Mes–acetylene (MesCCH). Using these substrates, the MCBD (**4–^{t}Bu**) and dMCBD (**5–Mes**) species of V were isolated, which are of particular importance for understanding the polymerization mechanism and their unique compositions.[27,35] In this paper, the labels **4–R** and **5–R** are used to denote putative or isolated MCBD and dMCBD species with various substitutions on the metallacycle, respectively, where R represents a ^{t}Bu, Mes, or Ph group.

Mechanistic Studies on the Formation of Cyclic Polymers and the Isolation of Potential Catalytic Intermediates. To investigate the initiation mechanism, we attempted to directly modulate the deprotonation of the MCBD intermediate: the reaction of the V-alkylidyne and alkyne monomer ^{t}BuCCH, containing a less acidic CH proton than PA, was chosen for this purpose. Treating complex **1–OEt$_2$** with an excess of the ^{t}BuCCH in toluene over several hours did not result in polymer formation. However, when using 3 equiv of ^{t}BuCCH in a toluene/benzene-d_6 mixture for 2 h at 50 °C, the MCBD complex (dBDI)V[C(^{t}Bu)C(H)C-(^{t}Bu)] (**4–^{t}Bu**) was formed and isolated in 79% yield relative to **1–OEt$_2$** (Scheme 2A). ^{1}H NMR spectral data of the reaction mixture indicated that complex **4–^{t}Bu** is not formed quantitatively under these conditions, and using a stoichiometric amount of the alkyne resulted in even lower yields.

Compound **4–^{t}Bu** has two characteristic resonances in its ^{1}H NMR spectrum (Figure S2) that correspond to the CH_2 fragment for the $dBDI^{2-}$ ligand backbone. These resonances appear at 3.01 and 3.74 ppm and are correlated to a single carbon negative contour at 81.5 ppm, observable in a ^{1}H–^{13}C{^{1}H} HSQC experiment (Figure S4). Additional ^{1}H–^{13}C{^{1}H} HSQC and HMBC (Figure S5) NMR spectroscopic experiments for **4–^{t}Bu** reveal coupling of the *β*-C***H*** (5.52 ppm) of the MCBD motif with the *β*-**C**H (96.4 ppm) and the *α*-**C**(^{t}Bu) atoms of the MCBD framework (144.3 and 163.6 ppm). Furthermore, the asymmetric nature of the $dBDI^{2-}$ ligand results in the system being C_1 symmetric, with the methine and methyl groups of the ^{i}Pr moieties being magnetically inequivalent. The combination of these spectral data confirms the stability of the MCBD unit in complex **4–^{t}Bu** and suggests deprotonation or proton migration does

https://doi.org/10.1021/jacs.3c08149
J. Am. Chem. Soc. 2024, 146, 2997−3009

not occur under the experimental conditions. Single-crystal X-ray diffraction (sc-XRD) analysis of **4−^{t}Bu** (Figure 3A and 3E) reveals the diamond-like structure of the MCBD scaffold, with short V−C_α (1.891(7) and 1.788(7) Å) and C_α−C_β distances (1.464(1) and 1.410(1) Å). Complex **4−^{t}Bu** exhibits bond distances akin to previously characterized MCBDs.[22,24,28,31,36,37] Although the V−C_β distance of 2.004(8) Å is shorter than the sum of their corresponding van der Waals atomic radii (3.71 Å),[38] there are no orbital interactions between V and C_β to suggest a strong covalent bond. The computed Mayer bond order of 0.32 between V and C_β indicates the absence of a strong covalent bond between these atoms (Figure S26b).[27]

To further explore the reactivity of V alkylidyne complex **1−OEt$_2$**, the reaction with a more sterically hindered aryl alkyne ,MesCCH, was investigated (Table S1). MesCCH has a predicted pK_a of 21.1, indicating its higher acidity compared to ^{t}BuCCH (pK_a ∼ 22.2, H_2O, 25 °C; calcd 22.3)[39] and PA (pK_a = 28.7, DMSO, 25 °C; calcd 20.3 in H_2O).[40] Under reaction conditions similar to those used for the formation of **4−^{t}Bu**, treating **1−OEt$_2$** with 3 equiv of MesCCH in toluene/benzene-d_6 at 50 °C did not yield a polymer. Instead, complex (BDI)V[C(^{t}Bu)CC(Mes)] (**5−Mes**) was isolated in 78% yield. Compound **5−Mes** lacks the characteristic CH_2 resonances of the dBDI^{2-} ligand with no negative contour observed in the ^{1}H−^{13}C{^{1}H} HSQC (Figure S11) NMR experiment. The absence of any sp^2 CH_2 group in **5−Mes** is further reflected in its C_s symmetric nature, as evidenced by the presence of only one methyl resonance consistent with a BDI$^-$ ligand (^{1}H NMR spectrum (Figure S8): 1.73 ppm). The ^{13}C{^{1}H} DEPT-135 NMR spectrum of **5−Mes** (Figure S20) further confirms the absence of methylene protons, indicating the protonation of dBDI^{2-} to BDI$^-$ and the deprotonation of the MCBD in **5−Mes**. Moreover, the methyl and methine protons of the isopropyl groups exhibit four (0.22, 0.63, 1.41, and 1.50 ppm) and two (1.03 and 4.24 ppm) resonances, respectively, with $^3J_{H-H}$ coupling constants of approximately 6.3 Hz, consistent with the assigned C_s symmetric nature of **5−Mes**. The structural and electronic differences of **4−^{t}Bu** and **5−Mes** are also reflected in their distinct ^{51}V NMR spectra, with resonances appearing at 251.6 and 1353.1 ppm for **4−^{t}Bu** (Figure S6) and **5−Mes** (Figure S13), respectively.

The sc-XRD data of **5−Mes** reveal two similar and relatively long V−C_α distances (V−C(Mes): 1.908(1) Å, V−C(^{t}Bu): 1.860(1) Å) in the dMCBD complex. The C_α−C_β distances (C(Mes)−C_β: 1.376(2) Å, and C(^{t}Bu)−C_β: 1.378(2) Å) are comparable, indicating that the C(^{t}Bu)CC(Mes) unit is bound to V as a formal 8e$^-$ donor and in an η^3-fashion (Figure 3B and 3E). The V−C_β distance of 1.967(1) Å is slightly shorter than that in **4−^{t}Bu**, suggesting a stronger interaction between these atoms in **5−Mes** and indicating a more puckered structure for the metallacycle (Figure 3D). This trend has also been observed for dMCBD when compared to their MCBD counterparts.[24,28,37,41] The C_α−C_β−C_α angle in **5−Mes** is 131.71(1)°, which is more obtuse compared to **4−^{t}Bu** (124.3(7)°) and similar to other structurally verified dMCBDs.[23] Based on the analogous acidities of MesCCH and PA, and considering the relative stability of compound **5−Mes**, it is possible that a similar dMCBD species, [(BDI)V-[C(^{t}Bu)CC(Ph)] (**5−Ph**), initiates the polymerization of PA. Density functional theory (DFT) computations suggest that the Gibbs free energy of dMCBD is 10.2 (**5−^{t}Bu**), 18.3 (**5−Mes**), and 13.7 kcal/mol (**5−Ph**), which are lower than those of their respective MCBD counterparts (Figure S26). It is proposed that the absence of the putative **5−^{t}Bu** species experimentally observed is due to steric hindrance from adjacent tertiary butyl groups, which prevents proton migration. The calculations indicate that the MCBD moiety in **5−Ph** is more fluxional and susceptible to a ring-opening mechanism compared to **5−Mes** (Figure S27). Additionally, it is demonstrated that the ring-opening mechanism plays a crucial role in enabling the coordination of PA monomers for the observed catalytic activity of V species (*vide infra*).

Interestingly, **5−Mes** can be independently obtained by using the conjugate acid of dBDI^{2-}, the BDI$^-$ ligand framework, in combination with the conjugate base of MesCCH, lithium mesitylide (LiCCMes). Specifically, a reaction between **2−OTf** and 1 equiv of LiCCMes at −35 °C in THF affords **5−Mes** in 58% yield (Scheme 2B). In contrast, the addition of excess ^{t}BuCCH or MesCCH to complex **2−OTf** does not induce [2+2]-cycloaddition even at elevated temperatures but rather leads to decomposition of **2−OTf**, as observed by ^{1}H NMR spectroscopy. Based on this difference in the reactivity of **1−OEt$_2$** and **2−OTf** in cycloaddition reactions with alkynes, it is hypothesized that the dissociation of OEt_2 from **1−OEt$_2$** is crucial for the cycloaddition of terminal alkyne to occur. This stark difference in reactivity between alkynes and **1−OEt$_2$** and **2−OTf** provides a hypothesis for the difference in polymerization activity and the mechanism for initiation. Complex **1−OEt$_2$** contains a site for protonation and readily facilitates proton transfer to form the dMCBD intermediate, which can then accept additional alkyne monomer units. On the other hand, the BDI$^-$ ligand V-alkylidyne **2−OTf** cannot accept a proton, thus preventing access to the dMCBD intermediate.

To further investigate the hypothesis of participation of dMCBD via proton transfer, the respective conjugate acid−base pairs of **1−OEt$_2$** and PA were examined. Treating **2−OTf** with 2 equiv of LiCCPh at −35 °C in THF resulted in the formation of a new compound in nearly quantitative yield (93% isolated yield). The verified structural identity of the complex is a doubly deprotio-metallacycle complex with a BDI$^-$ ligand, [Li(THF)$_4$][(BDI)V{C(Ph)CC(^{t}Bu)CC(Ph)}] (**6**) (Scheme 3). The use of stoichiometric amounts of LiCCPh yields **6** with unreacted **2−OTf**. In contrast, combining **1−OEt$_2$** and LiCCPh did not result in any reaction, even when the mixture was heated to 50 °C.

Compound **6** was characterized using multinuclear and multidimensional NMR spectroscopy and sc-XRD. In the ^{1}H NMR spectrum (Figure S15), the characteristic resonance of the methine γ-CH group in the ring of the BDI$^-$ ligand was observed at 5.76 ppm, which correlated to a carbon resonance at 97.41 ppm in the ^{1}H−^{13}C{^{1}H} HSQC NMR spectrum (Figure S18). The methyl groups of the BDI$^-$ β-carbons appeared as two separate resonances in the ^{1}H and ^{13}C{^{1}H} (Figure S16) NMR spectra ([1.60, 24.44] and [2.17, 25.65] ppm), indicating the lack of a mirror plane in complex **6** (C_1 symmetry). The methine (2.08, 3.18, 3.74, and 3.94 ppm) and methyl (−0.03, 1.09, 1.38, and 1.49 ppm) resonances of the ^{i}Pr moieties, exhibiting $^3J_{HH}$ coupling constants of ∼5.2 Hz, further confirmed the C_1 symmetric nature of the compound.

Single crystals of **6** suitable for sc-XRD study were obtained from a THF/hexane diffusion at −35 °C. The solid-state structure belongs to a monoclinic and centrosymmetric $P2_1/n$ space group. The structure reveals that the V−C_α bonds (1.914(2) and 1.985(2) Å) are longer than the respective

https://doi.org/10.1021/jacs.3c08149
J. Am. Chem. Soc. 2024, 146, 2997−3009

Scheme 3. Pathway to metallacycle species 6 and 6−H$^+$. [BAr$^F_4$]$^-$ = [B(C$_6$H$_3$(3,5-CF$_3$)$_2$)$_4$]$^-$, Ar = 2,6-^{i}Pr$_2$C$_6$H$_3$ along with the computed structure for catalytically active 6−H$^+$. Distances are reported in angstroms.

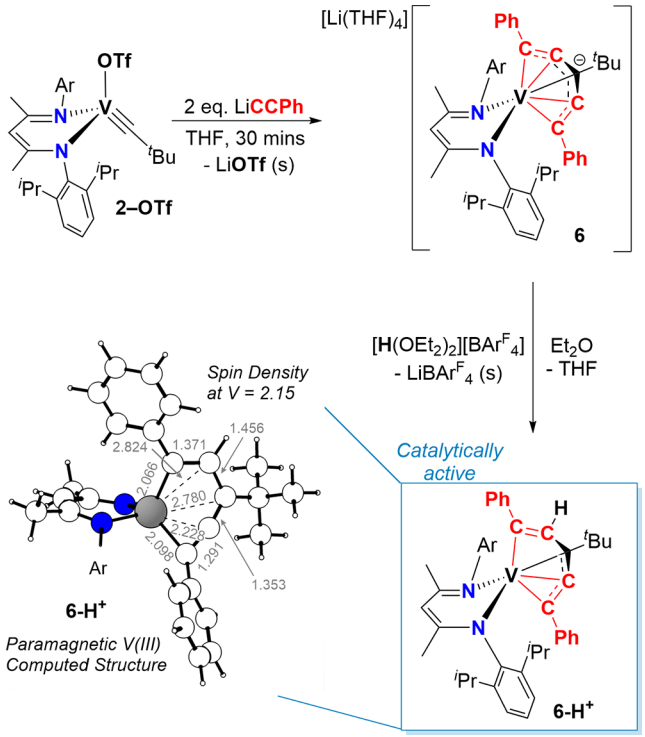

bonds found in both **4−^{t}Bu** and **5−Mes** (Figure 3E), indicative of the interaction between V and all carbons composing the doubly deprotio-metallacycle complex, **6**. The V−C$_\beta$ bond distances (2.038(2) and 2.014(2) Å) and V−C$_\gamma$ bond distances of 2.158(2) Å are all shorter than the sum of the van der Waals radii. The C$_5$R$_3$ motif (R = ^{t}Bu and two Ph) is best characterized as a trianionic ligand (6e$^-$ donor) bound to a low-spin V(III) center in an η^5 fashion. The V center dips below the C$_5$ ring by ∼1.03 Å, exhibiting to some extent a structural nonplanarity similar to the slippage of metal centers observed in most metallabenzenes.[42] Upon closer inspection, the five carbons representing the C$_5$R$_3$ fragment were found to be nearly planar, with the β-carbons slightly puckered by 0.093 and 0.193 Å from the imaginary plane composing the C$_\alpha$C$_\gamma$C$_\alpha$ atoms. The phenyl groups on the α-carbons deviate slightly from being orthogonal (74.5(4)°), and the planes of the two aryl groups on the β-diketiminate make an angle of 35.1(3)°, indicating the absence of notable symmetry elements in **6** (Figure 3C). In the case of the singlet state, DFT calculations reveal the presence of one doubly occupied d-dominated frontier orbital and four empty metal-dominated orbitals, while the triplet state shows two singly occupied and three empty d-orbitals in the frontier orbital domain (Figure S28), as shown in the Supporting Information, thus confirming the formal assignment of the V(III) oxidation state.

Route to Cyclic Polymers of Phenylacetylene (PA) Using Precursor 6. The formation of complex **6** from **2−OTf** and LiCCPh can shed light on the role of the BDI$^-$ ligand. Figure 4 presents a proposed mechanism for the formation of complex **6**, which incorporates DFT calculations and experimental observations. The reaction begins with the displacement of triflate by acetylide to form V(V)-alkylidyne

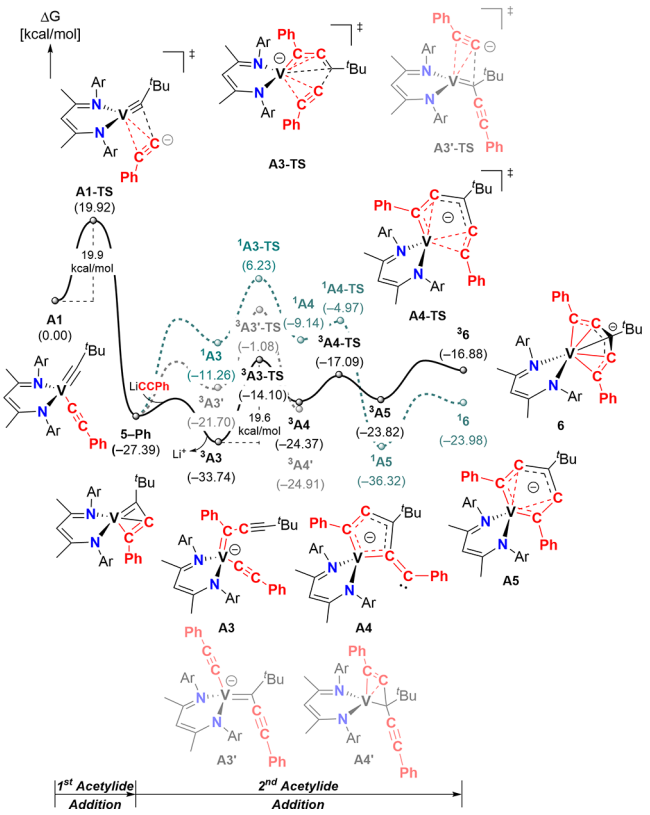

Figure 4. Proposed mechanism for the formation of **6**. Computational method: B3LYP-D3/LACV3P/cc-pVTZ(-f)//B3LYP-D3/LACVP/6-31G** with entropic corrections at −35 °C. Ar = 2,6-^{i}Pr$_2$C$_6$H$_3$.

species **A1**, accompanied by the precipitation of LiOTf (observed experimentally). Transition state **A1-TS**, representing a [2+2]-cycloaddition typical of alkyne metathesis,[27] leads to intermediate **5−Ph**. The barrier associated with **A1-TS** is 19.9 kcal/mol, and intermediate **5−Ph** releases −27.4 kcal/mol of free energy.

The second addition of LiCCPh occurred on the triplet electronic surface. Scheme 2G (*vide supra*) illustrates the plausible mechanism of electronic reorganization of **5−Ph** to ring-opened intermediate **5″−Ph**, which allows for the coordination of $^-$CCPh and the formation of intermediate **A3**. This metallacycle opening is formally a reductive elimination, and the metal center in **A3** adopts a V(III) oxidation state. In the presence of excess LiCCPh, the formation of **A3** is energetically preferred by 6.4 kcal/mol. Subsequently, intermediate **A3** undergoes a cyclization reaction to engage the three π-fragments, affording complex **A4**, as illustrated in Figure 4. This step traverses the transition state **A3-TS**, which is characterized as an alkynyl group transfer to the terminal end of the growing metallacycle fragment. Notably, the second addition of $^-$CCPh does not proceed through an η^2-type transition state, **^{3}A3′-TS**, because the reaction pathway requires the isomerization to a 12.0 kcal/mol higher energy isomer **^{3}A3′**, resulting in a barrier of 32.7 kcal/mol for this step. In comparison, the calculated barrier for the second acetylide addition via transition state **^{3}A3-TS** is 19.6 kcal/mol. Furthermore, this barrier is 0.3 kcal/mol lower than the barrier for the first acetylide addition, which leads to the formation of **5−Ph** (Figure 4). The implication of the lower barrier for the second LiCCPh addition is that the isolation of **5−Ph** under these reaction conditions is unlikely. Subsequent

https://doi.org/10.1021/jacs.3c08149
J. Am. Chem. Soc. 2024, 146, 2997−3009

rearrangement of the C_5R_3 ligand to adopt an η^4-bound structure gives complex **A5**, which exists in equilibrium with the η^5-bound isomer **6**. Energetically, the singlet states of **A5** and **6** are notably lower in energy than those of the triplet, as illustrated in Figure 4. Thus, our DFT calculations predict that the transformation of **5−Ph** to **6** proceeds through the triplet spin manifold, but the final product adopts the singlet spin state, which is consistent with the formal electron count and assignment of the electronic structure described above.

Complex **6** is inactive in polymerizing phenylacetylene (PA). However, the activity of its conjugate acid, **6−H$^+$**, in the formation of *c*-PPA was demonstrated by introducing a suitable proton source with a weakly coordinating anion. We hypothesized that neutralization of **6** with a H^+ would form a catalytically active species since its composition would be equivalent to **5−Ph** and PA. The addition of 1 equiv of Brookhart's acid, $[H(OEt_2)_2][BAr^F{}_{24}]$ ($[BAr^F{}_4]^-$ = $[B(C_6H_3(3,5\text{-}CF_3)_2)_4]^-$),[43] to **6** at −35 °C in diethyl ether resulted in an immediate color change from cherry-red to brown. After workup and removal of $[Li][BAr^F{}_{24}]$ and volatiles, a paramagnetic complex was obtained, as indicated by its broad resonances spanning −32 to 22 ppm in the ^{1}H NMR spectrum. Despite several attempts, the species that we propose to be (BDI)V{C(Ph)CHC(^{t}Bu)CC(Ph)} (**6−H$^+$**) could not be crystallized. Based on the proposed formation of **6−H$^+$** in Scheme 3, a solution magnetic moment susceptibility measurement was conducted using the Evans method, and this revealed a magnetic moment μ_{eff} = 2.71 μ_B (in C_6D_6, 300 K), consistent with a V(III)-d^2 high-spin system. Computational studies suggest that **6−H$^+$** is most stable in the triplet state with a Mulliken spin density of 2.15, which is suggestive of a high-spin V(III) center with two d-orbital-based valence electrons and some additional spin densities gained from the highly polarizable ligands, as depicted in Scheme 3. Thus, protonation inverts the energy ordering of the singlet and triplet states. Whereas the singlet state is preferred in the η^5-bound V(III) low-spin complex **6**, protonation leads to a significant weakening of the ligand field and an η^4-bound V(III) high-spin complex **6−H$^+$**.

Complex **6−H$^+$** was found to be active in catalyzing the polymerization of PA, resulting in the synthesis of cyclic poly(phenylacetylene), *c*-PPA. The polymer products obtained using **6−H$^+$** exhibit a longer elution time compared to their linear counterparts. This observation is consistent with the anticipated cyclic topology of *c*-PPA. The plot of log(molar mass) vs elution time demonstrates the difference in elution times between the synthesized polymers and linear poly(phenylacetylene) (*l*-PPA), further supporting their cyclic nature (Figure 2C and Table 1 entries 13−15 for reaction conditions). The SEC (size-exclusion chromatography) data indicate that the elution times of *c*-PPA synthesized using catalyst **6−H$^+$** do not overlap with those of *l*-PPA in the lower molar mass range. This suggests that the *c*-PPA obtained using **6−H$^+$** has fewer linear impurities compared to that of the *c*-PPA synthesized with catalyst **1−OEt$_2$** (Figure 2C and Table 1). It should be noted that while complex **6−H$^+$** is active in catalyzing the polymerization of PA, its activity is lower compared to **1−OEt$_2$**. However, the SEC data still confirm the successful synthesis of *c*-PPA with reduced amounts of linear impurities using catalyst **6−H$^+$**.

Proton Transfer to Form the dMCBD Scaffold in 5−Mes and Putative 5−Ph. The rearrangement of the MCBD scaffold to a dMCBD in complex **5−Mes** and the proposed **5−Ph** intermediate (Scheme 2B and F) raises questions about the mechanism of this transformation and the role of the BDI ligand in the polymerization. Similarly, the ability of **6−H$^+$** to catalyze the polymerization of PA into *c*-PPA suggests that an analogous intermediate with a BDI ligand may appear during the initial stages of polymerization when precatalyst **1−OEt$_2$** is used. To gain insight into these key mechanistic features, DFT calculations were performed starting from the presumed **4−Ph** structure formed upon the [2+2]-cycloaddition of PA to the alkylidyne ligand in **1−OEt$_2$** (Figure S25).

Calculations indicate that intermediate **4−Ph** may not undergo the subsequent PA addition step under the given reaction conditions. The calculated barrier for the PA addition to form a 6-membered vanadacycle intermediate, **5−Ph′**, is 45.0 kcal/mol, much too high for a reaction performed at room temperature. The main reason for this high barrier is the lack of access of the PA monomer to the vanadium center. The transition state of this outersphere mechanism involves the electrophilic addition of PA to the C_α of the cyclobutadiene without any assistance by the V-center (Figure 5).

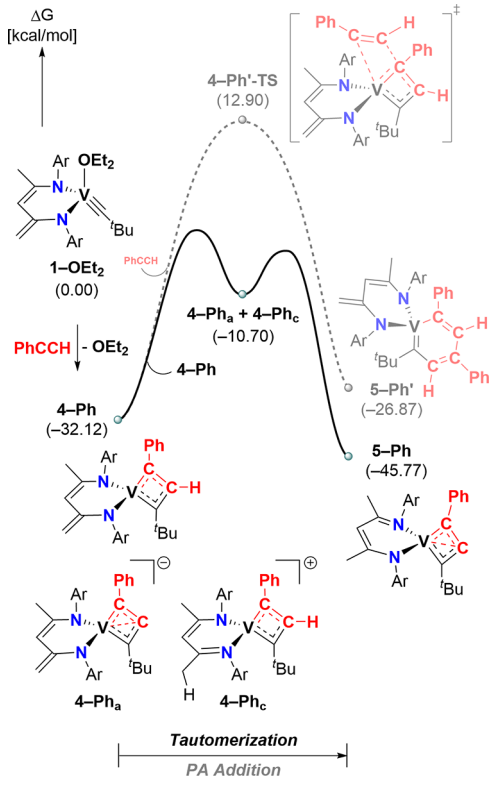

Figure 5. Tautomerization vs PA addition from **4−Ph**. Computational method: B3LYP-D3/LACV3P/cc-pVTZ(-f)//B3LYP-D3/LACVP/6-31G** with entropic contributions at 25 °C.

The mandatory addition of H^+ to the $dBDI^{2-}$ backbone to form **5−Mes** and the intermediate **5−Ph** demands that the MCBD resulting from [2+2]-cycloaddition of the terminal alkyne must relinquish a proton to the $dBDI^{2-}$ ligand. This tautomerization can be envisioned to proceed with the assistance of an external base, as illustrated in Figure 6A. Because the mechanistic role of such a base is to simply act as a proton shuttle, even **4−Ph** itself is a viable candidate. In this scenario, tautomerization could involve a bimolecular process where two molecules of **4−Ph** exchange proton and transform into the corresponding conjugate acid−base pairs (dBDI)V-

https://doi.org/10.1021/jacs.3c08149
J. Am. Chem. Soc. 2024, 146, 2997−3009

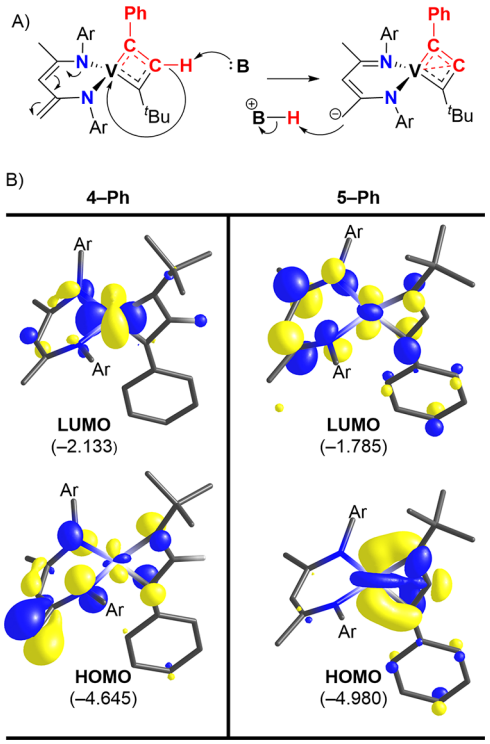

Figure 6. (A) Proposed mechanism for the tautomerization with the assistance of an external base. (B) Kohn–Sham orbitals, with isodensity values of 0.05 a.u., illustrate electronic reorganization due to tautomerization. Values in parentheses are the orbital energies in eV, Ar = 2,6-^{i}Pr$_2$C$_6$H$_3$.

[C(Ph)CC(Ph)] (**4–Ph$_a$**) and (BDI)V[C(Ph)CHC(Ph)] (**4–Ph$_c$**). These ion pairs can then combine and neutralize through a second proton exchange, leading to the formation of 2 equiv of **5–Ph** and release 35.1 kcal/mol of Gibbs free energy. The deprotonated form, **5–Ph**, is thermodynamically favored by 13.7 kcal/mol over the protonated form, e.g., **4–Ph** (Figure 5). Thus, self-promoted tautomerization is thermodynamically favorable.

Our calculations show that proton shuttling causes an electronic reorganization that significantly impacts the chemical reactivity. As illustrated in Figure 6B, the HOMO in **4–Ph** is delocalized over the BDI$^-$ ligand, whereas the LUMO features a nonbonding, in-plane d-orbital at vanadium, consistent with a V(V)-d^0 complex in which all nonbonding and M–L antibonding frontier orbitals are expected to be empty. During the tautomerization, the positive charge associated with the addition of the proton lowers the energies of all BDI-based orbitals, while the energies of orbitals located at the MCBD fragment increase due to the newly created negative charge associated with the proton loss at that site. The result of these energy shifts is that one of the BDI-based π^*-orbitals that was higher in energy than the metal-based LUMO in **4-Ph** becomes the LUMO in **5–Ph**. Likewise, the HOMO in **5–Ph** is one of the V–C σ-bonding orbitals that houses the valence electrons responsible for the σ-bonding interactions in the dMCBD moiety (Figure 6B). It is important to distinguish that the proton transfer is not associated with any redox event and the oxidation states of the metal and ligands remain unchanged; that is, the vanadium center maintains a formal V(V) oxidation state in both species.

The elevation of the orbital responsible for maintaining the V–C σ-bonding framework in the dMCBD fragment to the HOMO level weakens the metallacycle and gives access to a bent-allene complex **5′–Ph** and also an alkylidene-alkynyl species (**5″–Ph**), which is formed through a formal reductive elimination and, thus, features a V(III) center, as highlighted in Scheme 2G. Similar rearrangements were only speculated upon by Mortreux and co-workers in the formation of topologically undefined polymeric material from terminal alkynes and Schrock carbynes.[23] Although the precise identity of the active state of the catalyst remains unclear, these rearrangements are plausible. It is also notable that the UV–vis spectrum of **5–Mes** (Figure S34) features absorptions in the visible range with ε values in the range of 170–210 M^{-1} cm^{-1}, which may be assigned to be a d–d transition, which are reasonable for a V(III) intermediate. Beweries and co-workers have investigated the dMCBD on Ti(IV) complexes and have suggested that the bent-allene motif is not simply a dianionic ligand and the electronic modularity may invoke biradical character within the metallacycle.[44]

CONCLUSIONS

In conclusion, this work demonstrates for the first time that a vanadium alkylidyne such as **1–OEt$_2$** can polymerize PA and emphasizes the crucial role of ancillary ligands in the catalytic process. The polymers produced using these vanadium catalysts were found to be predominantly cyclic, showcasing the potential of this catalytic system for targeting interesting polymer topologies. By exploring the reaction of the conjugate acid of the vanadium alkylidyne, **1–OTf**, with the conjugate base of PA, $^-$CCPh, we identified and characterized the doubly deprotio-metallacycle complex, **6**. Upon protonation, this complex yields a neutral and paramagnetic complex, **6–H$^+$**, which exhibits catalytic activity for the polymerization of PA, resulting in cyclic polymers with minimal linear impurities.

The mechanism of vanadium-alkylidyne-catalyzed cyclic polymer formation from alkynes is still under investigation, but this work provides initial insights into the early stages of the reaction and the role of the dMCBD scaffold. Evidence supports the initiation of the polymerization through [2+2]-cycloaddition, as observed by the isolation of **4–^{t}Bu** from **1–OEt$_2$** and ^{t}BuCCH. However, with more acidic terminal alkynes such as MesCCH and PA, a different pathway is observed, involving an electronic and structural rearrangement accompanied by proton shuttling, which may be self-promoted through a bimolecular mechanism. The charge state of the BDI ligand that is controlled by the degree of protonation plays a crucial role in directing the ordering of the frontier orbitals, which in turn modulates the reactivity of the vanadium complex. These features offer an intriguing mechanistic variation to the traditional metathesis pathway.[22−25] Evidence for such a process is supported by the reaction of MesCCH with **1–OEt$_2$** to yield a dMCBD scaffold in **5–Mes**. The formation of the doubly deprotio-metallacycle complex, **6**, and the fact that its protonated derivative **6–H$^+$** is active in PA polymerization support the involvement of a cyclization mechanism in generating the cyclic polymers. In future work, these initial experimental observations and computational results will be refined and tested further to optimize the catalytic activity. This study opens up exciting avenues for the controlled synthesis of novel cyclic polymers and highlights the potential of early transition metal catalysts in this field.

https://doi.org/10.1021/jacs.3c08149
J. Am. Chem. Soc. 2024, 146, 2997–3009

■ ASSOCIATED CONTENT

Supporting Information

The Supporting Information is available free of charge at https://pubs.acs.org/doi/10.1021/jacs.3c08149.

General procedures, syntheses, NMR characterization, computational data, polymer topology, UV−vis and IR data, and X-ray crystallography data (PDF)

Accession Codes

CCDC 2249030−2249032 contain the supplementary crystallographic data for this paper. These data can be obtained free of charge via www.ccdc.cam.ac.uk/data_request/cif, or by emailing data_request@ccdc.cam.ac.uk, or by contacting The Cambridge Crystallographic Data Centre, 12 Union Road, Cambridge CB2 1EZ, UK; fax: +44 1223 336033.

■ AUTHOR INFORMATION

Corresponding Authors

Daniel J. Mindiola − *Department of Chemistry, University of Pennsylvania, Philadelphia, Pennsylvania 19104, United States;* orcid.org/0000-0001-8205-7868; Email: mindiola@sas.upenn.edu

Mu-Hyun Baik − *Center for Catalytic Hydrocarbon Functionalizations, Institute for Basic Science (IBS), Daejeon 34141, Republic of Korea; Department of Chemistry, Korea Advanced Institute of Science and Technology (KAIST), Daejeon 34141, Republic of Korea;* orcid.org/0000-0002-8832-8187; Email: mbaik2805@kaist.ac.kr

Adam S. Veige − *Department of Chemistry, Center for Catalysis, University of Florida, Gainesville, Florida 32611-7200, United States;* orcid.org/0000-0002-7020-9251; Email: veige@chem.ufl.edu

Brent S. Sumerlin − *Department of Chemistry, Center for Catalysis, University of Florida, Gainesville, Florida 32611-7200, United States;* orcid.org/0000-0001-5749-5444; Email: sumerlin@chem.ufl.edu

Authors

Mehrafshan G. Jafari − *Department of Chemistry, University of Pennsylvania, Philadelphia, Pennsylvania 19104, United States;* orcid.org/0000-0001-6807-7520

John B. Russell − *Department of Chemistry, University of Pennsylvania, Philadelphia, Pennsylvania 19104, United States;* orcid.org/0009-0004-3580-7610

Hanna Lee − *Department of Chemistry, Korea Advanced Institute of Science and Technology (KAIST), Daejeon 34141, Republic of Korea; Center for Catalytic Hydrocarbon Functionalizations, Institute for Basic Science (IBS), Daejeon 34141, Republic of Korea;* orcid.org/0000-0002-7391-6138

Bimal Pudasaini − *Center for Catalytic Hydrocarbon Functionalizations, Institute for Basic Science (IBS), Daejeon 34141, Republic of Korea*

Digvijayee Pal − *Department of Chemistry, Center for Catalysis, University of Florida, Gainesville, Florida 32611-7200, United States*

Zhihui Miao − *Department of Chemistry, Center for Catalysis, University of Florida, Gainesville, Florida 32611-7200, United States*

Michael R. Gau − *Department of Chemistry, University of Pennsylvania, Philadelphia, Pennsylvania 19104, United States;* orcid.org/0000-0002-4790-6980

Patrick J. Carroll − *Department of Chemistry, University of Pennsylvania, Philadelphia, Pennsylvania 19104, United States*

Complete contact information is available at: https://pubs.acs.org/10.1021/jacs.3c08149

Author Contributions

All authors have given approval to the final version of the manuscript.

Funding

We thank the U.S. National Science Foundation (CHE-0848248, CHE-1152123, and CHE-2108266) and the University of Pennsylvania for the financial support of this research. The authors also acknowledge the NIH supplement awards 3R01GM118510-03S1 and 3R01GM087605-06S1 and financial support of the Vagelos Institute for Energy Sciences and Technology for the purchase of NMR instrument NEO600. J.B.R. thanks the Vagelos Institute for Energy Science and Technology (VIEST) for a predoctoral fellowship. The computational part of this research was financially supported by the Institute for Basic Science in Korea (IBS-R10-A1).

Notes

The authors declare no competing financial interest.

■ ACKNOWLEDGMENTS

We dedicate this work to the late Professor Robert Grubbs.

■ ABBREVIATIONS

acac,acetylacetonate; COD,1,5-cyclooctadiene; PA,phenylacetylene; *c*-PPA,cyclic poly(phenylacetylene); *l*-PPA,linear poly(phenylacetylene); BDI^{-},*β*-diketiminate ligand, $[ArNC(CH_3)]_2CH^{-}$ (Ar = 2,6-$^{i}Pr_2C_6H_3$); $dBDI^{2-}$,deprotonated *β*-diketiminate, $[ArNC(CH_3)CHC(CH_2)NAr]^{2-}$ (Ar = 2,6-$^{i}Pr_2C_6H_3$); MCBD,metallacyclobutadiene; dMCBD,deprotio-metallacyclobutadiene; Mes,mesityl; ^{t}Bu,*tert*-butyl; sc-XRD,single-crystal X-ray diffraction; PCM,polarizable continuum model; SEC,size-exclusion chromatography

■ REFERENCES

(1) Liu, J.; Lam, J. W. Y.; Tang, B. Z. Acetylenic Polymers: Syntheses, Structures, and Functions. *Chem. Rev.* **2009**, *109* (11), 5799−5867.

(2) Nakagawa, T.; Saito, T.; Asakawa, S.; Saito, Y. Polyacetylene derivatives as membranes for gas separation. *Gas Sep. Purif.* **1988**, *2* (1), 3−8.

(3) Shirakawa, H. Synthesis and characterization of highly conducting polyacetylene. *Synth. Met.* **1995**, *69* (1), 3−8.

(4) Iyoda, M.; Yamakawa, J.; Rahman, M. J. Conjugated Macrocycles: Concepts and Applications. *Angew. Chem., Int. Ed.* **2011**, *50* (45), 10522−10553.

(5) Lam, J. W. Y.; Tang, B. Z. Functional Polyacetylenes. *Acc. Chem. Res.* **2005**, *38* (9), 745−754. Ohn, N.; Kim, J. G. Mechanochemical Post-Polymerization Modification: Solvent-Free Solid-State Synthesis of Functional Polymers. *ACS Macro Lett.* **2018**, *7* (5), 561−565.

(6) Haque, F. M.; Grayson, S. M. The synthesis, properties and potential applications of cyclic polymers. *Nat. Chem.* **2020**, *12* (5), 433−444.

(7) (a) Orrah, D. J.; Semlyen, J. A.; Ross-Murphy, S. B. Studies of cyclic and linear poly(dimethylsiloxanes): 28. Viscosities and densities of ring and chain poly(dimethylsiloxane) blends. *Polymer* **1988**, *29* (8), 1455−1458. (b) Garcia Bernal, J. M.; Tirado, M. M.; Freire, J. J.; Garcia de La Torre, J. Monte Carlo calculation of hydrodynamic

properties of linear and cyclic polymers in good solvents. *Macromolecules* **1991**, *24* (2), 593−598.
(8) (a) Zimm, B. H.; Stockmayer, W. H. The Dimensions of Chain Molecules Containing Branches and Rings. *J. Chem. Phys.* **1949**, *17* (12), 1301−1314. (acccessed 2020/05/23) (b) Benmounaa, M.; Maschke, U. Theoretical Aspects of Cyclic Polymers: Effects of Excluded Volume Interactions. In *Cyclic Polymers*; Semlyen, J. A., Ed.; Springer: Netherlands, 2002; pp 741−790.
(9) (a) Griffiths, P. C.; Stilbs, P.; Yu, G. E.; Booth, C. Role of molecular architecture in polymer diffusion: a PGSE-NMR study of linear and cyclic poly (ethylene oxide). *J. Phys. Chem.* **1995**, *99* (45), 16752−16756. (b) Santangelo, P. G.; Roland, C. M.; Chang, T.; Cho, D.; Roovers, J. Dynamics near the Glass Temperature of Low Molecular Weight Cyclic Polystyrene. *Macromolecules* **2001**, *34* (26), 9002−9005.
(10) Divandari, M.; Morgese, G.; Ramakrishna, S. N.; Benetti, E. M. Surface-grafted assemblies of cyclic polymers: Shifting between high friction and extreme lubricity. *Eur. Polym. J.* **2019**, *110*, 301−306.
(11) Bielawski, C. W.; Benitez, D.; Grubbs, R. H. An "Endless" Route to Cyclic Polymers. *Science* **2002**, *297* (5589), 2041.
(12) Laurent, B. A.; Grayson, S. M. Synthetic approaches for the preparation of cyclic polymers. *Chem. Soc. Rev.* **2009**, *38* (8), 2202−2213.
(13) (a) Jia, Z.; Monteiro, M. J. Cyclic polymers: Methods and strategies. *J. Polymer Sci. Part A: Polymer Chem.* **2012**, *50* (11), 2085−2097. (b) Chang, Y. A.; Waymouth, R. M. Recent progress on the synthesis of cyclic polymers via ring-expansion strategies. *J. Polymer Sci. Part A: Polymer Chem.* **2017**, *55* (18), 2892−2902.
(14) (a) Corey, E. J.; Hamanaka, E. A New Synthetic Approach to Medium-Size Carbocyclic Systems. *J. Am. Chem. Soc.* **1964**, *86* (8), 1641−1642. (b) Schmalz, H.-G. Catalytic Ring-Closing Metathesis: A New, Powerful Technique for Carbon−Carbon Coupling in Organic Synthesis. *Angew. Chem. Int. Ed., Eng.* **1995**, *34* (17), 1833−1836. (c) Schrock, R. R. Multiple Metal−Carbon Bonds for Catalytic Metathesis Reactions (Nobel Lecture). *Angew. Chem., Int. Ed.* **2006**, *45* (23), 3748−3759. (d) Pasini, D. The click reaction as an efficient tool for the construction of macrocyclic structures. *Molecules* **2013**, *18* (8), 9512−9530. (e) Pangilinan, K.; Advincula, R. Cyclic polymers and catenanes by atom transfer radical polymerization (ATRP). *Polym. Int.* **2014**, *63* (5), 803−813.
(15) (a) Boydston, A. J.; Xia, Y.; Kornfield, J. A.; Gorodetskaya, I. A.; Grubbs, R. H. Cyclic Ruthenium-Alkylidene Catalysts for Ring-Expansion Metathesis Polymerization. *J. Am. Chem. Soc.* **2008**, *130* (38), 12775−12782. (b) Xia, Y.; Boydston, A. J.; Yao, Y.; Kornfield, J. A.; Gorodetskaya, I. A.; Spiess, H. W.; Grubbs, R. H. Ring-Expansion Metathesis Polymerization: Catalyst-Dependent Polymerization Profiles. *J. Am. Chem. Soc.* **2009**, *131* (7), 2670−2677. (c) Kricheldorf, H. R. Cyclic polymers: Synthetic strategies and physical properties. *J. Polym. Sci., Part A: Polym. Chem.* **2010**, *48* (2), 251−284.
(16) Nadif, S. S.; Kubo, T.; Gonsales, S. A.; VenkatRamani, S.; Ghiviriga, I.; Sumerlin, B. S.; Veige, A. S. Introducing "Ynene" Metathesis: Ring-Expansion Metathesis Polymerization Leads to Highly Cis and Syndiotactic Cyclic Polymers of Norbornene. *J. Am. Chem. Soc.* **2016**, *138* (20), 6408−6411.
(17) (a) Sarkar, S.; McGowan, K. P.; Kuppuswamy, S.; Ghiviriga, I.; Abboud, K. A.; Veige, A. S. An OCO^{3-} Trianionic Pincer Tungsten(VI) Alkylidyne: Rational Design of a Highly Active Alkyne Polymerization Catalyst. *J. Am. Chem. Soc.* **2012**, *134* (10), 4509−4512. (b) McGowan, K. P.; O'Reilly, M. E.; Ghiviriga, I.; Abboud, K. A.; Veige, A. S. Compelling mechanistic data and identification of the active species in tungsten-catalyzed alkyne polymerizations: conversion of a trianionic pincer into a new tetraanionic pincer-type ligand. *Chem. Sci.* **2013**, *4* (3), 1145−1155. (c) Roland, C. D.; Li, H.; Abboud, K. A.; Wagener, K. B.; Veige, A. S. Cyclic polymers from alkynes. *Nat. Chem.* **2016**, *8* (8), 791−796. (d) Niu, W.; Gonsales, S. A.; Kubo, T.; Bentz, K. C.; Pal, D.; Savin, D. A.; Sumerlin, B. S.; Veige, A. S. Polypropylene: Now Available without Chain Ends. *Chem.* **2019**, *5* (1), 237−244. (e) Roland, C. D.; Zhang, T.; VenkatRamani, S.; Ghiviriga, I.; Veige, A. S. A catalytically relevant intermediate in the synthesis of cyclic polymers from alkynes. *Chem. Commun.* **2019**, *55* (91), 13697−13700. (f) Miao, Z.; Pal, D.; Niu, W.; Kubo, T.; Sumerlin, B. S.; Veige, A. S. Cyclic Poly(4-methyl-1-pentene): Efficient Catalytic Synthesis of a Transparent Cyclic Polymer. *Macromolecules* **2020**, *53* (18), 7774−7782. (g) Miao, Z.; Gonsales, S. A.; Ehm, C.; Mentink-Vigier, F.; Bowers, C. R.; Sumerlin, B. S.; Veige, A. S. Cyclic polyacetylene. *Nat. Chem.* **2021**, *13* (8), 792−799. (h) Sueyoshi, S.; Taniguchi, T.; Tanaka, S.; Asakawa, H.; Nishimura, T.; Maeda, K. Understanding the Polymerization of Diphenylacetylenes with Tantalum(V) Chloride and Cocatalysts: Production of Cyclic Poly(diphenylacetylene)s by Low-Valent Tantalum Species Generated in Situ. *J. Am. Chem. Soc.* **2021**, *143* (39), 16136−16146.
(18) Basuli, F.; Bailey, B. C.; Brown, D.; Tomaszewski, J.; Huffman, J. C.; Baik, M.-H.; Mindiola, D. J. Terminal Vanadium−Neopentylidyne Complexes and Intramolecular Cross-Metathesis Reactions to Generate Azametalacyclohexatrienes. *J. Am. Chem. Soc.* **2004**, *126* (34), 10506−10507.
(19) Adhikari, D.; Basuli, F.; Orlando, J. H.; Gao, X.; Huffman, J. C.; Pink, M.; Mindiola, D. J. Zwitterionic and Cationic Titanium and Vanadium Complexes Having Terminal M−C Multiple Bonds. The Role of the β-Diketiminate Ligand in Formation of Charge-Separated Species. *Organometallics* **2009**, *28* (14), 4115−4125.
(20) Trhlíková, O.; Zedník, J.; Balcar, H.; Brus, J.; Sedláček, J. [Rh(cycloolefin)(acac)] complexes as catalysts of polymerization of aryl- and alkylacetylenes: Influence of cycloolefin ligand and reaction conditions. *J. Mol. Catal. A: Chem.* **2013**, *378*, 57−66.
(21) (a) Semlyen, J. A.; Semlyen, E. R. Cyclic Polymers; Springer Netherlands, 2000. Hoskins, J. N.; Grayson, S. M. Cyclic polyesters: synthetic approaches and potential applications. *Polymer Chem.* **2011**, *2* (2), 289−299. (b) Roovers, J.; Toporowski, P. M. Synthesis of high molecular weight ring polystyrenes. *Macromolecules* **1983**, *16* (6), 843−849.
(22) (a) Fürstner, A.; Davies, P. W. Alkyne metathesis. *Chem. Commun.* **2005**, No. 18, 2307−2320. (b) Fürstner, A. Alkyne Metathesis on the Rise. *Angew. Chem., Int. Ed.* **2013**, *52* (10), 2794−2819.
(23) (a) Beer, S.; Hrib, C. G.; Jones, P. G.; Brandhorst, K.; Grunenberg, J.; Tamm, M. Efficient Room-Temperature Alkyne Metathesis with Well-Defined Imidazolin-2-iminato Tungsten Alkylidyne Complexes. *Angew. Chem., Int. Ed.* **2007**, *46* (46), 8890−8894. (b) Zhang, W.; Moore, J. S. Alkyne Metathesis: Catalysts and Synthetic Applications. *Adv. Syn. Catal.* **2007**, *349* (1−2), 93−120. (c) Heppekausen, J.; Stade, R.; Kondoh, A.; Seidel, G.; Goddard, R.; Fürstner, A. Optimized Synthesis, Structural Investigations, Ligand Tuning and Synthetic Evaluation of Silyloxy-Based Alkyne Metathesis Catalysts. *Chem.—Eur. J.* **2012**, *18* (33), 10281−10299. (d) Estes, D. P.; Gordon, C. P.; Fedorov, A.; Liao, W.-C.; Ehrhorn, H.; Bittner, C.; Zier, M. L.; Bockfeld, D.; Chan, K. W.; Eisenstein, O.; et al. Molecular and Silica-Supported Molybdenum Alkyne Metathesis Catalysts: Influence of Electronics and Dynamics on Activity Revealed by Kinetics, Solid-State NMR, and Chemical Shift Analysis. *J. Am. Chem. Soc.* **2017**, *139* (48), 17597−17607. (e) Ehrhorn, H.; Bockfeld, D.; Freytag, M.; Bannenberg, T.; Kefalidis, C. E.; Maron, L.; Tamm, M. Studies on Molybdena- and Tungstenacyclobutadiene Complexes Supported by Fluoroalkoxy Ligands as Intermediates of Alkyne Metathesis. *Organometallics* **2019**, *38* (7), 1627−1639. (f) Cui, M.; Bai, W.; Sung, H. H. Y.; Williams, I. D.; Jia, G. Robust Alkyne Metathesis Catalyzed by Air Stable d2 Re(V) Alkylidyne Complexes. *J. Am. Chem. Soc.* **2020**, *142* (31), 13339−13344. (g) Hauser, P. M.; van der Ende, M.; Groos, J.; Frey, W.; Wang, D.; Buchmeiser, M. R. Cationic Tungsten Alkylidyne N-Heterocyclic Carbene Complexes: Synthesis and Reactivity in Alkyne Metathesis. *Eur. J. Inorg. Chem.* **2020**, *2020* (32), 3070−3082. (h) Fürstner, A. The Ascent of Alkyne Metathesis to Strategy-Level Status. *J. Am. Chem. Soc.* **2021**, *143* (38), 15538−15555. (i) Haack, A.; Hillenbrand, J.; van Gastel, M.; Fürstner, A.; Neese, F. Spectroscopic and Theoretical Study on Siloxy-Based Molybdenum and Tungsten Alkylidyne Catalysts for Alkyne Metathesis. *ACS Catal.* **2021**, *11* (15), 9086−9101. (j) Haack,

https://doi.org/10.1021/jacs.3c08149
J. Am. Chem. Soc. 2024, 146, 2997−3009

A.; Hillenbrand, J.; Leutzsch, M.; van Gastel, M.; Neese, F.; Fürstner, A. Productive Alkyne Metathesis with "Canopy Catalysts" Mandates Pseudorotation. *J. Am. Chem. Soc.* **2021**, *143* (15), 5643−5648. (k) Ge, Y.; Huang, S.; Hu, Y.; Zhang, L.; He, L.; Krajewski, S.; Ortiz, M.; Jin, Y.; Zhang, W. Highly active alkyne metathesis catalysts operating under open air condition. *Nat. Commun.* **2021**, *12* (1), 1136. (l) Hillenbrand, J.; Korber, J. N.; Leutzsch, M.; Nöthling, N.; Fürstner, A. Canopy Catalysts for Alkyne Metathesis: Investigations into a Bimolecular Decomposition Pathway and the Stability of the Podand Cap. *Chem.—Eur. J.* **2021**, *27* (56), 14025−14033. (m) Cui, M.; Sung, H. H. Y.; Williams, I. D.; Jia, G. Alkyne Metathesis with d2 Re(V) Alkylidyne Complexes Supported by Phosphino-Phenolates: Ligand Effect on Catalytic Activity and Applications in Ring-Closing Alkyne Metathesis. *J. Am. Chem. Soc.* **2022**, *144* (14), 6349−6360. (n) Bittner, C.; Ehrhorn, H.; Bockfeld, D.; Brandhorst, K.; Tamm, M. Tuning the Catalytic Alkyne Metathesis Activity of Molybdenum and Tungsten 2,4,6-Trimethylbenzylidyne Complexes with Fluoroalkoxide Ligands OC(CF3)nMe3−n (n = 0−3). *Organometallics* **2017**, *36* (17), 3398−3406.

(24) Ehrhorn, H.; Tamm, M. Well-Defined Alkyne Metathesis Catalysts: Developments and Recent Applications. *Chem.—Eur. J.* **2019**, *25* (13), 3190−3208.

(25) Schrock, R. R. High-oxidation-state molybdenum and tungsten alkylidyne complexes. *Acc. Chem. Res.* **1986**, *19* (11), 342−348.

(26) (a) Churchill, M. R.; Ziller, J. W. Crystal structure of (η5-C5H5)W[C(Ph)C(CMe3)C(Ph)]Cl2, a molecule possessing a localized, non-planar tungstenacyclobutadiene ring. *J. Organomet. Chem.* **1985**, *279* (3), 403−412. (b) Beer, S.; Brandhorst, K.; Hrib, C. G.; Wu, X.; Haberlag, B.; Grunenberg, J.; Jones, P. G.; Tamm, M. Experimental and Theoretical Investigations of Catalytic Alkyne Cross-Metathesis with Imidazolin-2-iminato Tungsten Alkylidyne Complexes. *Organometallics* **2009**, *28* (5), 1534−1545. (c) O'Reilly, M. E.; Ghiviriga, I.; Abboud, K. A.; Veige, A. S. Unusually stable tungstenacyclobutadienes featuring an ONO trianionic pincer-type ligand. *Dalton Trans.* **2013**, *42* (10), 3326−3336. (d) Ramírez-Contreras, R.; Bhuvanesh, N.; Ozerov, O. V. Cycloaddition and C−H Activation Reactions of a Tantalum Alkylidyne. *Organometallics* **2015**, *34* (7), 1143−1146. (e) Cui, M.; Lin, R.; Jia, G. Chemistry of Metallacyclobutadienes. *Chem.—Asian J.* **2018**, *13* (8), 895−912. (f) Bai, W.; Lee, K.-H.; Sung, H. H. Y.; Williams, I. D.; Lin, Z.; Jia, G. Alkyne Metathesis Reactions of Rhenium(V) Carbyne Complexes. *Organometallics* **2016**, *35* (22), 3808−3815. (g) Schrock, R. R.; Weinstock, I. A.; Horton, A. D.; Liu, A. H.; Schofield, M. H. Preparation of rhenium(VII) monoimido alkylidyne complexes and metathesis of acetylenes via rhenacyclobutadiene intermediates. *J. Am. Chem. Soc.* **1988**, *110* (8), 2686−2687.

(27) Suresh, C. H.; Frenking, G. 1,3-Metal−Carbon Bonding and Alkyne Metathesis: DFT Investigations on Model Complexes of Group 4, 5, and 6 Transition Metals. *Organometallics* **2012**, *31* (20), 7171−7180.

(28) McCullough, L. G.; Listemann, M. L.; Schrock, R. R.; Churchill, M. R.; Ziller, J. W. Multiple metal-carbon bonds. 34. Why terminal alkynes cannot be metathesized. Preparation and crystal structure of a deprotonated tungstacyclobutadiene complex, W(η5-C5H5)[C3(CMe3)2]Cl. *J. Am. Chem. Soc.* **1983**, *105* (22), 6729−6730.

(29) McCullough, L. G.; Schrock, R. R.; Dewan, J. C.; Murdzek, J. C. Multiple metal-carbon bonds. 38. Preparation of trialkoxymolybdenum(VI) alkylidyne complexes, their reactions with acetylenes, and the X-ray structure of Mo[C3(CMe3)2][OCH(CF3)-2](C5H5N)2. *J. Am. Chem. Soc.* **1985**, *107* (21), 5987−5998.

(30) Strutz, H.; Dewan, J. C.; Schrock, R. R. Multiple metal-carbon bonds. 40. Reaction of Mo(CCMe3)[OCH(CF3)2]3-(dimethoxyethane) with tert-butylacetylene, an aborted acetylene polymerization. *J. Am. Chem. Soc.* **1985**, *107* (21), 5999−6005.

(31) Freudenberger, J. H.; Schrock, R. R. Multiple metal-carbon bonds. 42. Formation of tungstenacyclobutadiene complexes containing a proton in the ring and their conversion to deprotio tungstenacyclobutadiene complexes. *Organometallics* **1986**, *5* (7), 1411−1417.

(32) Haberlag, B.; Freytag, M.; Daniliuc, C. G.; Jones, P. G.; Tamm, M. Efficient Metathesis of Terminal Alkynes. *Angew. Chem., Int. Ed.* **2012**, *51* (52), 13019−13022.

(33) Bray, A.; Mortreux, A.; Petit, F.; Petit, M.; Szymanska-Buzar, T. Metathesis vs. Polymerization of terminal acetylenes over [W(CBut)-(OBut)3]. *J. Chem. Soc., Chem. Commun.* **1993**, *2*, 197−199.

(34) (a) Casey, C. P.; Kraft, S.; Powell, D. R. [1,3]-Metal Shifts in Rhenium Alkynyl Carbene Complexes. *Organometallics* **2001**, *20* (13), 2651−2653. (b) Lhermet, R.; Fürstner, A. Cross-Metathesis of Terminal Alkynes. *Chem.—Eur. J.* **2014**, *20* (41), 13188−13193.

(35) (a) Bursten, B. E. On the stability of early-transition-metal metallacyclobutadiene complexes. *J. Am. Chem. Soc.* **1983**, *105* (1), 121−122. (b) Lugo, A.; Fischer, J.; Lawson, D. B. Titanacyclobutadiene: structure, properties, and relative stability. *Journal of Molecular Structure: THEOCHEM* **2004**, *674* (1), 139−146.

(36) (a) Wengrovius, J. H.; Sancho, J.; Schrock, R. R. Metathesis of acetylenes by tungsten(VI)-alkylidyne complexes. *J. Am. Chem. Soc.* **1981**, *103* (13), 3932−3934. (b) Schrock, R. R.; Freudenberger, J. H.; Listemann, M. L.; McCullough, L. G. Recent advances in the chemistry of well-defined olefin and acetylene metathesis catalysts. *J. Mol. Catal.* **1985**, *28* (1−3), 1−8. (c) Strutz, H.; Dewan, J.; Schrock, R. Multiple metal-carbon bonds. 40. Reaction of Mo (CCMe3)[OCH (CF3)2]3(dimethoxyethane) with tert-butylacetylene, an aborted acetylene polymerization. *J. Am. Chem. Soc.* **1985**, *107* (21), 5999−6005. (d) Schrock, R. R. Living ring-opening metathesis polymerization catalyzed by well-characterized transition-metal alkylidene complexes. *Acc. Chem. Res.* **1990**, *23* (5), 158−165. (e) Weiss, K.; Goller, R.; Loessel, G. Investigations of polymerisation and metathesis reactions: Part XII: Alkene metathesis and alkyne polymerisation with the carbyne complex Cl_3 (dme) W≡ $CCMe_3$. *J. Mol. Catal.* **1988**, *46* (1−3), 267−275.

(37) McCullough, L. G.; Schrock, R. R.; Dewan, J. C.; Murdzek, J. C. Preparation of trialkoxymolybdenum (VI) alkylidyne complexes, their reactions with acetylenes, and the x-ray structure of Mo[C3 (CMe3)2][OCH(CF3)2](C5H5N)2. *J. Am. Chem. Soc.* **1985**, *107* (21), 5987−5998.

(38) Batsanov, S. S. Van der Waals Radii of Elements. *Inorg. Material* **2001**, *37* (9), 871−885.

(39) Kresge, A. J.; Pruszynski, P.; Stang, P. J.; Williamson, B. L. Base-catalyzed hydrogen exchange and estimates of the acid strength of benzoyl-and (trimethylsilyl) acetylene in aqueous solution. A correlation between acetylene pKa estimates and hydroxide ion catalytic coefficients for hydrogen exchange. *J. Org. Chem.* **1991**, *56* (15), 4808−4811.

(40) Bordwell, F. G.; Drucker, G. E.; Andersen, N. H.; Denniston, A. D. Acidities of hydrocarbons and sulfur-containing hydrocarbons in dimethyl sulfoxide solutions. *J. Am. Chem. Soc.* **1986**, *108* (23), 7310−7313.

(41) Heppekausen, J.; Stade, R.; Kondoh, A.; Seidel, G.; Goddard, R.; Fürstner, A. Optimized Synthesis, Structural Investigations, Ligand Tuning and Synthetic Evaluation of Silyloxy-Based Alkyne Metathesis Catalysts. *Chem.—Eur. J.* **2012**, *18* (33), 10281−10299.

(42) Zhu, J.; Jia, G.; Lin, Z. Understanding Nonplanarity in Metallabenzene Complexes. *Organometallics* **2007**, *26* (8), 1986−1995.

(43) Brookhart, M.; Grant, B.; Volpe, A. F., Jr. [(3,5-(CF3)-2C6H3)4B]-[H(OEt2)2]+: a convenient reagent for generation and stabilization of cationic, highly electrophilic organometallic complexes. *Organometallics* **1992**, *11* (11), 3920−3922.

(44) Reiß, F.; Reiß, M.; Bresien, J.; Spannenberg, A.; Jiao, H.; Baumann, W.; Arndt, P.; Beweries, T. 1-Titanacyclobuta-2,3-diene − an elusive four-membered cyclic allene. *Chem. Sci.* **2019**, *10* (20), 5319−5325.

(45) Russell, J. B.; Konar, D.; Keller, T.; Gau, M. R.; Carroll, P. J.; Telser, J.; Lester, D. W.; Veige, A. S.; Sumerlin, B. S.; Mindiola, D. J. Metallacyclobuta-(2,3)-diene: A Bidentate Ligand for Stream-line Synthesis of First Row Transition Metal Catalysts for Cyclic

https://doi.org/10.1021/jacs.3c08149
J. Am. Chem. Soc. 2024, 146, 2997−3009

Polymerization of Phenylacetylene. *Angew. Chem. Int. Ed.* **2024**, e202318956.

https://doi.org/10.1021/jacs.3c08149
J. Am. Chem. Soc. 2024, 146, 2997−3009